

Effect of the Turbulent Oil Film on the Dynamic Characteristics of Two-lobe Journal Bearings

Stanisław Kazimierz STRZELECKI 

Lodz University of Technology

Łódź, Poland; e-mail: stanislaw.strzelecki@p.lodz.pl

Turbogenerators in power plants utilize two-lobe journal bearings, which can carry large loads with good stability at the speeds typically encountered in the power industry. These bearings feature the profiles such as elliptical, offset, cylindrical or pericycloidal. The design of these bearings ensures proper load capacity, favorable thermal conditions for the oil film, and stable operation of the associated turbounits. However, the design of these bearings should be supported by calculations that account for turbulence generated in the oil film.

This paper presents the results of dynamic characteristic calculations for four types of two-lobe journal bearings operating under adiabatic laminar or turbulent flow conditions in the lubricating gap. The dynamic characteristics, expressed as the stiffness and damping coefficients of the oil film, were obtained using the perturbation method. Stability ranges for a simple symmetric rotor were determined for the considered bearings. A numerical algorithm for the iterative solution of the Reynolds, energy and viscosity equations was employed to calculate the oil film forces, which formed the basis for the bearing's dynamic characteristics. These investigations were carried out assuming the static equilibrium position of the journal.

Keywords: multilobe journal bearing; turbulent oil film; dynamic characteristics; rotor stability.



Copyright © 2025 The Author(s).

Published by IPPT PAN. This work is licensed under the Creative Commons Attribution License CC BY 4.0 (<https://creativecommons.org/licenses/by/4.0/>).

1. INTRODUCTION

Journal bearings designers are increasingly encountering situations where turbulent operation occurs with increasing regularity [1–5]. This is primarily due to the use of process fluids with low kinematic viscosity as lubricants, as well as the higher surface speeds of the journals being experienced. Turbulent lubrication theory is required in the design of oil-lubricated journal and thrust bearings in large powers generation equipment, water-lubricated journal bearings for boiler feed pumps, and seals in advanced gas turbine engines.

Durable, reliable and robust rotating machines – particularly turbounits – are characterized by large specific loads and rotational speeds that result in

high efficiency. This means that journal bearings often become a limiting factor in their design [4–6]. The rotors of turbomachinery typically operate in two- and three-lobe journal bearings, ensuring operation at the assumed temperature, minimizing power losses, and maintaining good rotor stability. Some designs of turbo machines also incorporate tilting-pad bearings [7, 8].

Turbulent velocities generate extreme shear gradients at the surface of the bearing and journal, which is very important in the context of thermo-elasto-hydrodynamic lubrication (TEHD) [2]. In addition to the increased viscous shear, the apparent boost in viscosity reduces the flow of lubricant, thereby raising its temperature levels. At very high journal speeds, thermal effects become significant. However, these effects alone cannot predict bearing performances, thus the effect of turbulence has to be considered.

Currently, three turbulent lubrication theories are available to bearings designers [9–11]; these theories enable the investigation of high-speed bearing operation. In order to calculate the performances of such bearings, the Reynolds and energy equations have to include the terms that account for the turbulence generated in the oil film. The applied turbulence model should include transitional and Taylor vortex flows.

The developed numerical algorithm for calculating journal bearings includes the turbulence coefficients [3, 12]; this algorithm allows for the calculations of both static and dynamic characteristics for different types of journal bearings with arbitrary sleeve profiles. The turbulence coefficients must be computed numerically [1, 3].

The aim of this paper is to determine the dynamic characteristics of two-lobe journal bearings operating with either a laminar or turbulent oil film. The Reynolds, energy and viscosity equations were solved numerically using the finite differences method, with the application of turbulence correction factors. It was assumed that there was either an adiabatic laminar or turbulent oil film, with parallel alignment of the journal and sleeve axes, as well as the static equilibrium positions for the journal. The dynamic characteristics, specifically the stiffness and damping coefficients of the oil film, were obtained by the perturbation method. Stability ranges for a simple symmetric rotor operating in the considered journal bearings were also determined.

2. GEOMETRY, REYNOLDS AND ENERGY EQUATIONS

Typical two-lobe journal bearings can be composed of single circular sections whose center of curvature are either located at (Fig. 1a, c) or not located at (Fig. 1b, d) the geometric center of the bearing. The multilobe cylindrical (Fig. 1a) and pericycloid (Fig. 1c) journal bearings (“wave bearings”) [12] are

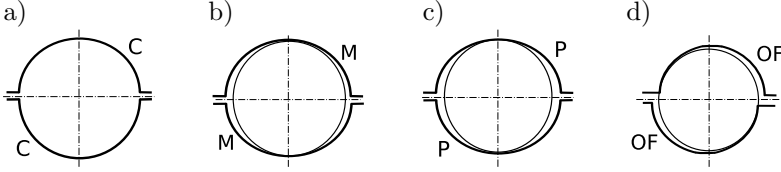


FIG. 1. Multilobe journal bearings with two lobes and different profiles: 2C – cylindrical (a), 2M – classic (b-discontinuous), 2P – pericycloid (c-continuous profile), 2OF – offset (d).

characterized by a continuous profile. In contrast, the geometric configuration of the bearing, shown in Fig. 1b and Fig. 1d, is a whole discontinuous.

Assuming parallel axes of the journal and bearing sleeve, the geometry of the oil film gap in a multilobe journal bearing (Fig. 2) is described by Eq. (2.1); the first term of this equation provides the geometry of a multilobe bearing [2, 3, 12].

$$(2.1) \quad \bar{H}(\varphi) = \bar{H}_{Li}(\varphi) - \varepsilon \cdot \cos(\varphi - \alpha),$$

where $\bar{H} = h/(R-r)$ – dimensionless oil film thickness, h – oil film thickness [m], R, r – sleeve and journal radii [m], α – attitude angle [°], ε – relative eccentricity, and φ – peripheral co-ordinate.

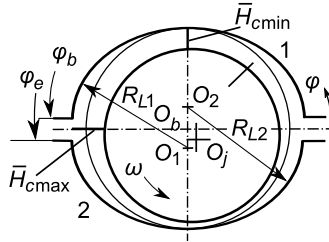


FIG. 2. Geometry of two-lobe journal bearings; R_{L1}, R_{L2} – radii of lobe 1 and 2, respectively, $O_b, O_{1,2}, O_j$ – centers of the sleeve, lobe and journal, R_p – radius of pericycloid, 1, 2, 3 – lobe numbers, – minimum and maximum oil film thickness at central position of the journal, respectively.

Multilobe and pericycloid bearings' geometries are described by Eq. (2.2) and Eq. (2.3), respectively.

$$(2.2) \quad \bar{H}_{Li}(\varphi) = \psi_{si} + (\psi_{si} - 1) \cdot \cos(\varphi - \gamma_i),$$

where γ_i is the angle of lobe center point, and ψ_{si} is the lobe relative clearance.

$$(2.3) \quad \bar{H}_P(\varphi) = \lambda^*(1 + \cos n_p \varphi),$$

where λ^* is the pericycloid relative eccentricity, and n_p is the multiple of the pericycloid.

Figure 3 exemplarily presents the oil film thickness of two-lobe, compatible bearings [12]: multilobe and pericycloid journal bearings at the central position of the journal in the sleeve. The relations of pericycloid eccentricity λ^* and lobe relative clearance ψ_{si} are also shown in Fig. 3.

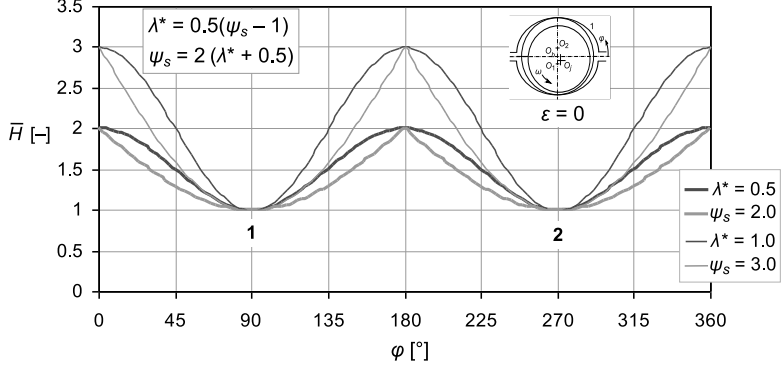


FIG. 3. Comparison of oil film thickness of two-lobe compatible journal bearings: multilobe and pericycloid at the center position of the journal in the sleeve [1].

The oil film pressure and temperature-viscosity fields were determined using the Reynolds, energy and viscosity equations, derived under the assumption of adiabatic, laminar or turbulent flow of non-compressible Newtonian fluid in the bearing gap [2, 12]. The Reynolds Eq. (2.4) and the transformed energy Eq. (2.5) include the correlation factors of turbulence.

$$(2.4) \quad \frac{\partial}{\partial \varphi} \left(\frac{\bar{H}^3}{\bar{\eta} K_x} \frac{\partial \bar{p}}{\partial \varphi} \right) + \frac{\partial}{\partial \bar{z}} \left(\frac{\bar{H}^3}{\bar{\eta} K_z} \frac{\partial \bar{p}}{\partial \bar{z}} \right) = 6 \frac{\partial \bar{H}}{\partial \varphi} + 12 \frac{\partial \bar{H}}{\partial \varphi},$$

where \bar{H} – dimensionless oil film thickness, \bar{p} – dimensionless pressure, φ , z – peripheral and axial coordinates, K_x , K_z – turbulence correlation factors, $\phi = \omega t$ – dimensionless time, $\bar{\eta}$ – dimensionless oil viscosity, and ω – angular velocity.

$$(2.5) \quad \frac{1}{\bar{\eta}} \frac{\partial \bar{T}}{\partial \varphi} = \frac{K_t \int_{-L/D}^{L/D} \left[\frac{\bar{\tau}_c}{\bar{H}} + \frac{\bar{H}^3}{12\bar{\eta}^2} \left(\frac{1}{K_x} \left(\frac{\partial \bar{p}}{\partial \varphi} \right)^2 + \frac{1}{K_z} \left(\frac{\partial \bar{p}}{\partial \bar{z}} \right)^2 \right) \right] d\bar{z}}{\int_{-L/D}^{L/D} \left(\frac{\bar{H}}{2} - \frac{\bar{H}^3}{12\bar{\eta}} \frac{\partial \bar{p}}{\partial \varphi} \right) d\bar{z}},$$

where thermal coefficient $K_t = \omega \eta_0 / (c_t \rho g T_0 \psi^2)$, c_t – specific heat of oil [J/(kg · K)], T_0 – supplied oil temperature [°C], η_0 – dynamic viscosity of supplied oil [N · s/m²], ρ – oil density [kg/m³], and $\bar{\tau}_c$ – correlation factor for shearing stresses [12].

The viscosity $\bar{\eta}$, which must be determined, and the pressure gradients $\frac{\partial \bar{p}}{\partial \varphi}$, $\frac{\partial \bar{p}}{\partial \bar{z}}$ are on the right side of Eq. (2.5). Therefore, the oil film temperature, viscosity, pressure $\bar{p}(\varphi, \bar{z})$, and the correlation factor coefficients K_x , K_z , for turbulent flow must be determined through an iterative process [1, 9].

3. STABILITY OF A SIMPLE SYMMETRIC ROTOR OPERATING IN TWO-LOBE JOURNAL BEARINGS

The transformation of the equations of motion for the journal and the center of the elastic, symmetrically supported rotor yields its real and imaginary parts [13]. Further considerations allow for obtaining the characteristic equation of the 6th order (3.1) with respect to λ [13].

$$(3.1) \quad c_6 \lambda^6 + c_5 \lambda^5 + c_4 \lambda^4 + c_3 \lambda^3 + c_2 \lambda^2 + c_1 \lambda + c_0 = 0.$$

The assumed solution of Eq. (3.1) is $\lambda_j = -u_j + iv_j$ ($1 \leq j \leq 6$), where u represents damping and v represents the self-vibrations. The stability of the linear vibrations of system occurs only when all real parts of the eigenvalues λ_j are negative. The coefficients c_0 through c_6 in Eq. (3.1) are the functions of a_0 , b_0 , g_{ik} , b_{ik} (3.2):

$$(3.2) \quad c_0 \div c_6 = f(a_0, b_0, g_{ik}, b_{ik}),$$

where a_0 – ratio of angular velocity ω to the angular self-frequency of stiff shaft, $a_0 = (\omega/\omega_c)^2$, ω_c – angular self-frequency of stiff rotor, $\omega_c = \sqrt{c^*/m}$, b_0 – ratio of the Sommerfeld number to the relative elasticity of the shaft, $b_0 = S_0/c_s$, c^* – shaft stiffness [N/m], c_s – relative elasticity of the shaft, $c_s = f/\Delta R = g/(\omega_c^2 \cdot \Delta R)$, f – static deflection of shaft [m], F – resultant force of the oil film [N], F_{stat} – static load of the bearing [N], g – acceleration due to gravity [m/s²], g_{ik} – dimensionless stiffness coefficients, $g_{ik} = S_0[\Delta R/F_{\text{stat}}]$, g'_{ik} – stiffness coefficients [N/m], b_{ik} – dimensionless damping coefficients, $b_{ik} = S_0[\Delta R/F_{\text{stat}}]\omega \cdot b'_{ik}$, b'_{ik} – damping coefficients [N · s/m], m – mass of the rotor [kg], and S_0 – the Sommerfeld number, $S_0 = F \cdot \psi^2 / (L \cdot D \cdot \eta \cdot \omega)$.

The coefficients of the characteristic frequency equation of 6th order [4] depend on the stiffness g_{ik} , damping b_{ik} coefficients, the Sommerfeld number S_0 , the relative elasticity of the shaft c_s and the ratio of angular velocity to the critical angular velocity of the stiff rotor. As a result of these transformations, the expression determining the ratio of boundary angular speed Ω_b to the critical angular speed ω_c , as well as the stability of the rotor, has the following form [12–16]:

$$(3.3) \quad \left(\frac{\Omega_b}{\omega_c} \right) = \frac{1}{1 + b_0 \cdot \frac{A_3}{A_1}} \frac{A_2 \cdot A_3^2}{A_1^2 + A_1 \cdot A_3 \cdot A_4 + A_0 \cdot A_3^2},$$

where A_0 through A_4 are combinations of four stiffness coefficients g_{ik} and four damping coefficients b_{ik} [1]:

$$\begin{aligned} A_0 &= g_{11}b_{22} - g_{12}b_{21}, & A_1 &= g_{11}b_{22} + g_{22}b_{11} - g_{12}b_{21} - g_{21}b_{12}, \\ A_2 &= b_{11}b_{22} - b_{12}b_{21}, & A_3 &= b_{11} + b_{22}, & A_4 &= g_{11} + g_{22}. \end{aligned}$$

4. RESULTS OF CALCULATIONS

The dynamic characteristics in the form of stiffness and damping coefficients, as well as the stability regions of a simple symmetric rotor, are presented in Fig. 4 through Fig. 14. It was assumed that the bearing length-to-diameter ratio is $L/D = 1$ with a relative clearances $\psi = 1.2\text{‰}$ and lobe relative clearances, $\psi_s = 1$ (for the 2C configuration) and $\psi_s = 3$ (for the 2M and 2OF configurations), and ψ_s (for the 2P configuration). The rotational speed of the journal was 4000 rpm, and the supplied oil temperature was $T_0 = 40^\circ\text{C}$. The Reynolds numbers were: the critical $Re_{cr} = 2600$ and $Re = 4398$ for turbulent flow in the bearing gap at the assumed rotational speed of the journal in the bearing. The thermal coefficient was $K_t = 0.055$ for the assumed operating conditions of the bearing.

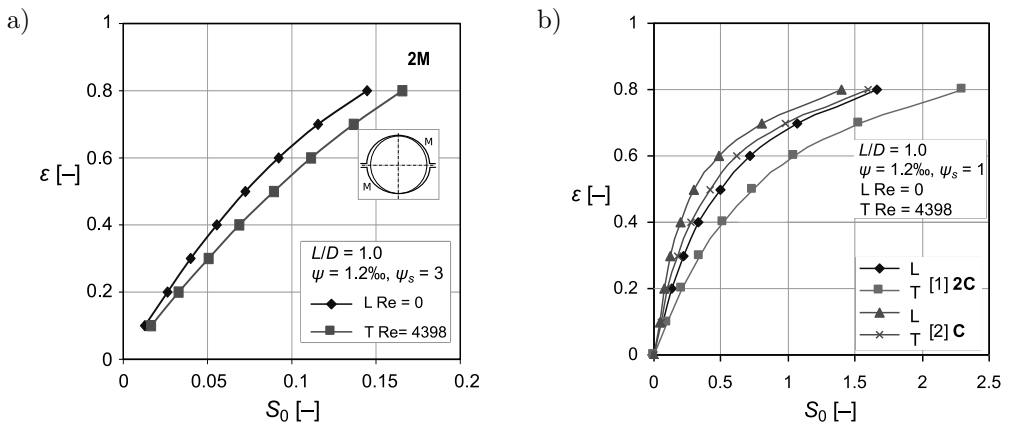


FIG. 4. Relative eccentricity versus the Sommerfeld number for two-lobe journal bearings under laminar (L) and turbulent (T) oil film conditions: a) 2M bearing, b) comparison of C and 2C bearings.

Figure 4 shows one of the static characteristics of the bearing: the relative eccentricity versus the Sommerfeld number for two-lobe journal bearings under both laminar and turbulent oil film conditions. For all considered bearings, the load capacity is higher in the turbulent case than in the laminar case. Turbulence results in an increase in the load capacity at an assumed relative eccentricity of the journal. For example, at a relative eccentricity $\varepsilon = 0.6$ there is an increase

from $S_0 = 0.7$ to $S_0 = 1.1$ (Fig. 4a). These findings align with results obtained by HAN [3], who also observed an increase in load capacity; for instance, at $\varepsilon = 0.6$, $S_0 = 0.5$ increased to $S_0 = 0.6$ – for a cylindrical bearing, too. In this investigation, an increase in S_0 for the 2C bearing, specifically, at $\varepsilon = 0.6$ was observed, rising from $S_0 = 0.7$ to $S_0 = 1.1$ (Fig. 4b). Although both authors considered two different types of bearings, the trends of the curves and the observed increases are similar (with both the 2C and C showing similar behavior in the range of S_0 up to 2.4).

The stiffness g_{ik} and damping b_{ik} coefficients of the two-lobe (2C, cylindrical lobes) journal bearing operating with laminar and turbulent oil film are given in Fig. 5 and Fig. 6, respectively. It can be observed that stiffness coefficients g_{11} , g_{12} , g_{21} (Fig. 5) and the damping coefficients b_{11} , b_{12} , b_{21} (Fig. 6) have very close

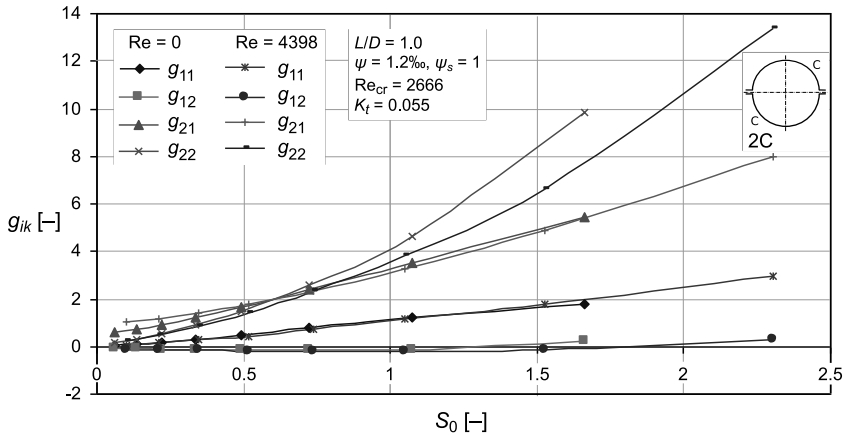


FIG. 5. Stiffness coefficients of two-lobe (2C, cylindrical lobes) journal bearing operating with laminar and turbulent oil films.

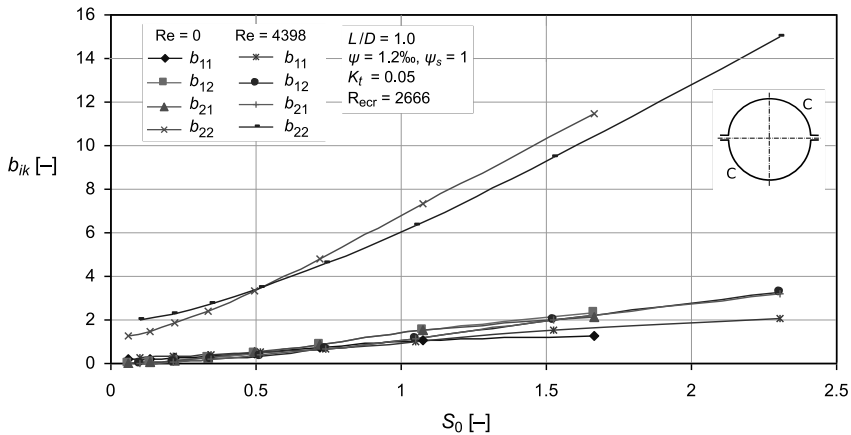


FIG. 6. Damping coefficients of two-lobe (2C, cylindrical lobes) journal bearing operating with laminar and turbulent oil films.

values for both types of oil flow in the bearing gap. The stiffness coefficient g_{22} for both types of flow shows almost the same values up to a Sommerfeld number $S_0 = 0.6$, but beyond this value, g_{22} for laminar flow is larger than for turbulent flow (Fig. 5). The damping coefficient b_{22} for laminar flow is slightly smaller than b_{22} for turbulent flow up to a Sommerfeld number $S_0 \approx 0.6$; but, at S_0 increases, the trend reverses (Fig. 6).

The values of stiffness (Fig. 7) and damping (Fig. 8) coefficients for the two-lobe (2M, multilobe two-lobe) journal bearing vary depending on the type of oil film (laminar or turbulent). The coefficients g_{11} and g_{21} (Fig. 7) have very similar values, while g_{12} with negative values for both types of flow, is larger for laminar flow. The coefficient g_{22} shows larger values for turbulent oil flow (Fig. 7). The damping coefficients b_{11} , b_{22} , (Fig. 6) are also larger for turbulent oil

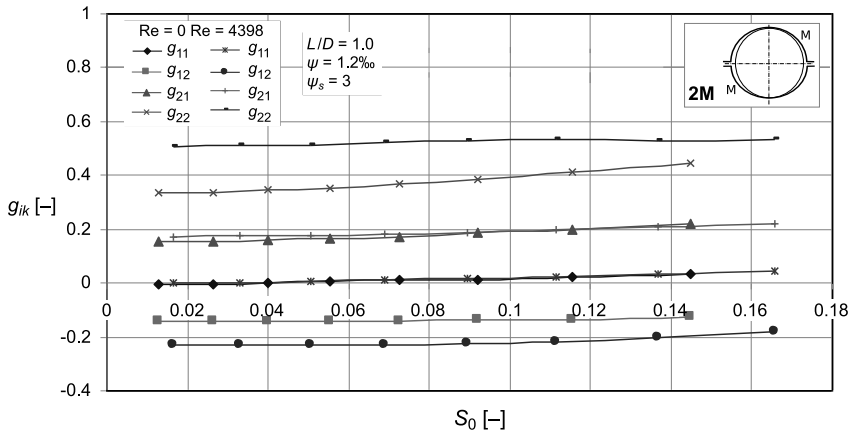


FIG. 7. Stiffness coefficients of two-lobe (2M, multilobe lobes) journal bearings operating with laminar and turbulent oil films.

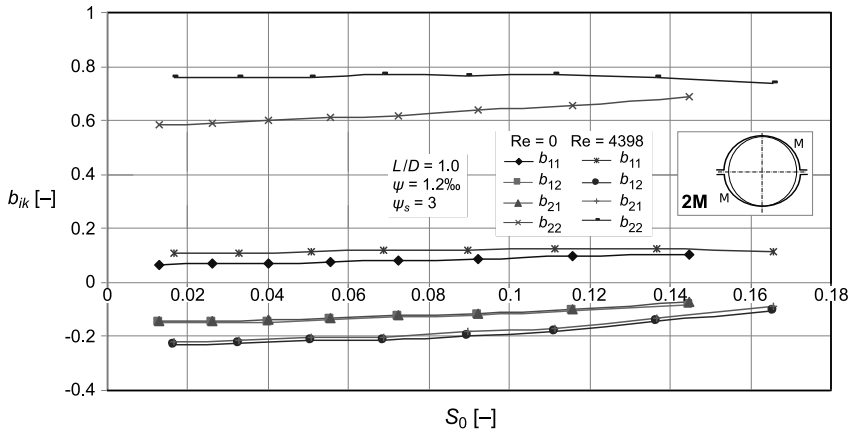


FIG. 8. Damping coefficients of two-lobe (2M, multilobe lobes) journal bearings operating with laminar and turbulent oil films.

flow. The coupled coefficients b_{12} and b_{21} have very close negative values, but this coefficients are larger in the case of laminar oil flow in the bearing gap (Fig. 8).

There is a significant difference in the values of load capacity S_0 and the behavior of all coefficients between the two-lobe cylindrical (2C) and 2M bearings, with the latter showing a more parallel trend (e.g., Fig. 5 and Fig. 7). Usually, the bearings with a cylindrical sleeve profile are characterized by higher load capacity compared to multilobe bearings. However, cylindrical bearings tend to have lower stability at higher operating speeds and are more susceptible to oil whirl [2, 12].

Figures 9 and 10 show the stiffness and damping coefficients of the two-lobe bearing (2OF, offset lobes). This type of bearing is commonly applied in high speed, heavy-duty turbine gearboxes as bearings for the input shaft [12]. They provide both good load capacity and stability at high operating speed [8, 12].

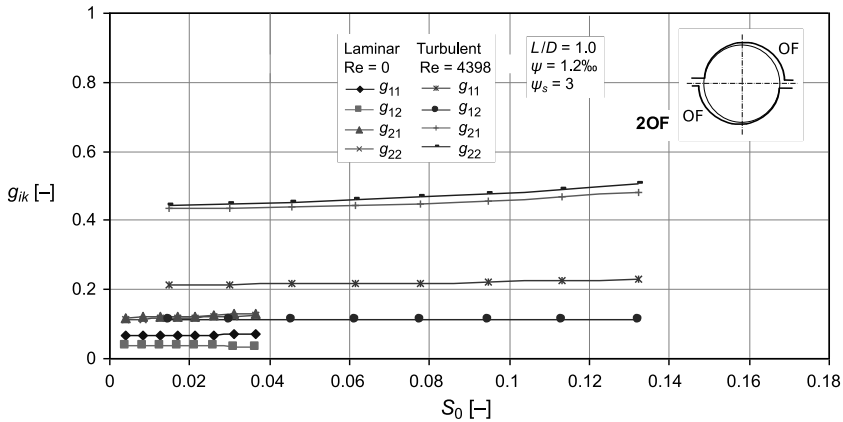


FIG. 9. Stiffness coefficients of two-lobe (2OF, offset lobes) journal bearings operating with laminar and turbulent oil films.

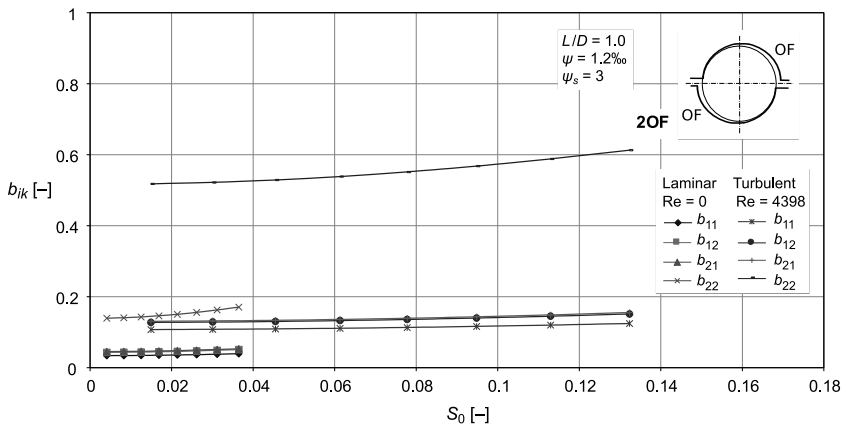


FIG. 10. Damping coefficients of two-lobe (2OF, offset lobes) journal bearings operating with laminar and turbulent oil films.

The range of load capacity is significantly smaller under laminar flow (where S_0 varies from 0 to 0.039) than under turbulent flow (where S_0 varies from 0.01 to 0.13). All stiffness and damping coefficients are larger for the turbulent case (e.g., Fig. 9, g_{11} or g_{22} , and Fig. 10, b_{11} , b_{22}). In terms of stiffness coefficients, there are large differences between g_{21} and g_{22} for laminar and turbulent oil flows (Fig. 9). The large difference among the damping coefficients is shown by the coefficient b_{22} , which ranges from 0.52 to 0.61 for turbulent oil flow and from 0.12 up to 0.19 for laminar oil film (Fig. 10). The coupled coefficients b_{12} and b_{21} are equal in both oil flow cases. All stiffness and damping coefficients are positive (e.g., Fig. 10).

The stiffness and damping coefficients of the two-lobe pericycloid (2P) journal bearing are shown in Fig. 11 and Fig. 12, respectively. In the case of turbulent

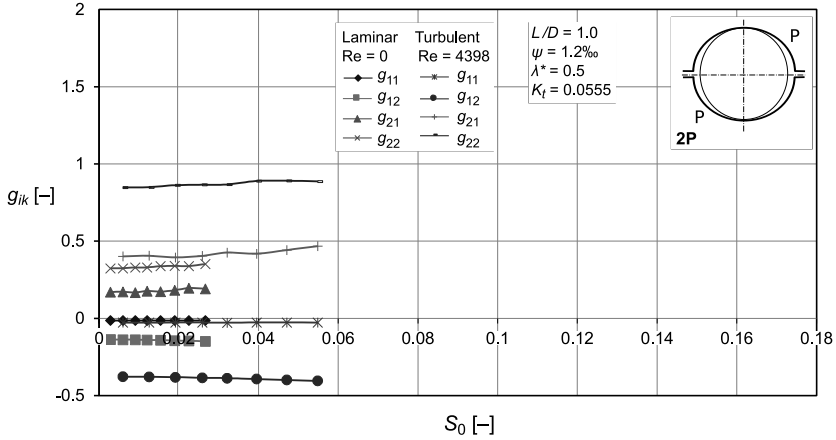


FIG. 11. Stiffness coefficients of two-lobe (2P, multilobe, pericycloid lobes) journal bearing operating with laminar and turbulent oil films.

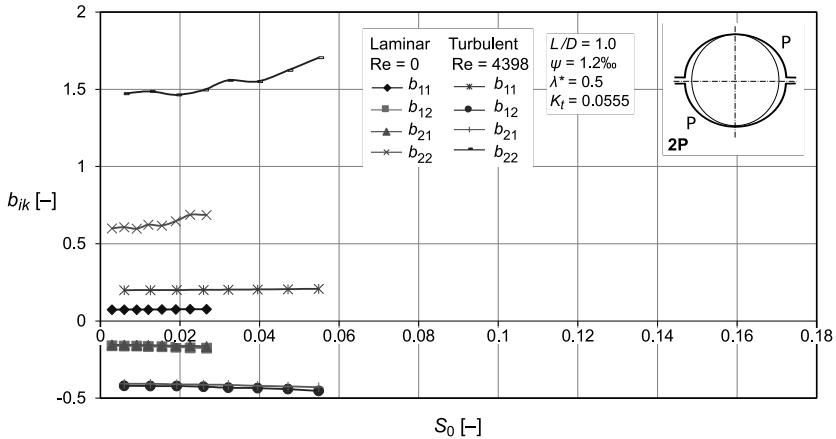


FIG. 12. Damping coefficients of two-lobe (2P, multilobe, pericycloid lobes) journal bearing operating with laminar and turbulent oil films.

oil film, all dynamic coefficients exhibit in larger range of the Sommerfeld number. The range of S_0 is from zero up to 0.028 for the laminar case, while S_0 for the turbulent case ranges from zero to 0.058. The coefficient g_{11} has similar negative values for both cases of oil flow; however, it is in a smaller range of load capacity for laminar flow (Fig. 11). Coefficients g_{21} , g_{22} are larger for the turbulent film, but g_{12} is larger for the laminar case. Damping coefficients b_{11} and b_{22} (Fig. 12, with the largest differences observed for the coefficient b_{22}) are larger for the turbulent film, while the coupled coefficients b_{12} and b_{21} are negative and larger for the laminar flow. In both oil flow conditions, the coupled coefficients are characterized by similar values (e.g., Fig. 12, b_{12} and b_{21} for turbulent oil film).

Figure 13 shows a comparison of chosen stiffness g_{11} , g_{22} and damping b_{11} , b_{22} coefficients for the two-lobe (2M) journal bearing operating with laminar and turbulent oil films. The coefficient g_{11} has, for both flow types, very similar values up to $S_0 = 0.069$; however, beyond this value, g_{11} is slightly larger for turbulent flow. In contrast, g_{22} , b_{11} , b_{22} are all larger in the case of turbulent flow.

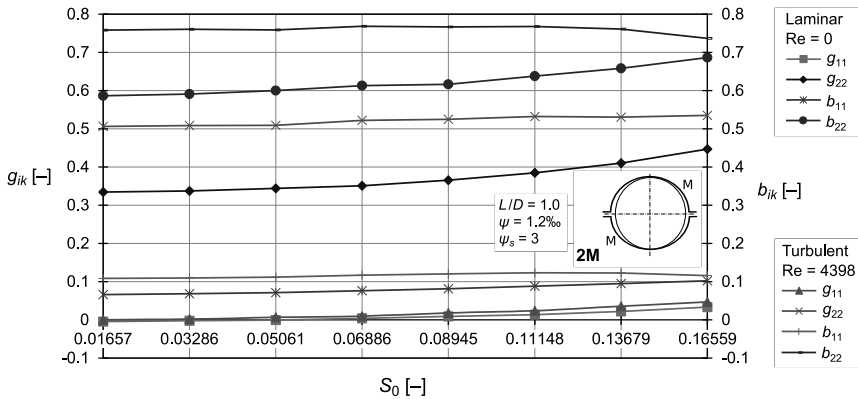


FIG. 13. Comparison of the stiffness and damping coefficients of the two-lobe (2M, multilobe) journal bearing operating with laminar and turbulent oil films.

The stability ranges of a simple symmetric rotor operating in different types of two-lobe journal bearings versus the critical Sommerfeld number are shown in Fig. 14 (S_{0c} – the critical Sommerfeld number, $S_{0c} = S_0\omega/\omega_c$). The coefficient $\text{tg } \tau$ (Fig. 14) is the measure of stability properties of the bearing [2, 4]. Larger values of the angle τ indicate a larger stability range, meaning that at the assumed load, there is a higher boundary number of revolutions Ω_b/ω_c [13].

For the considered two-lobe bearing (2M), the rotor stability and curve behavior are similar (Fig. 14). However, the stability ranges are different; in the case of turbulent flow (Fig. 14b) in bearing gap, the angle τ is smaller than for the laminar flow case (Fig. 14a).

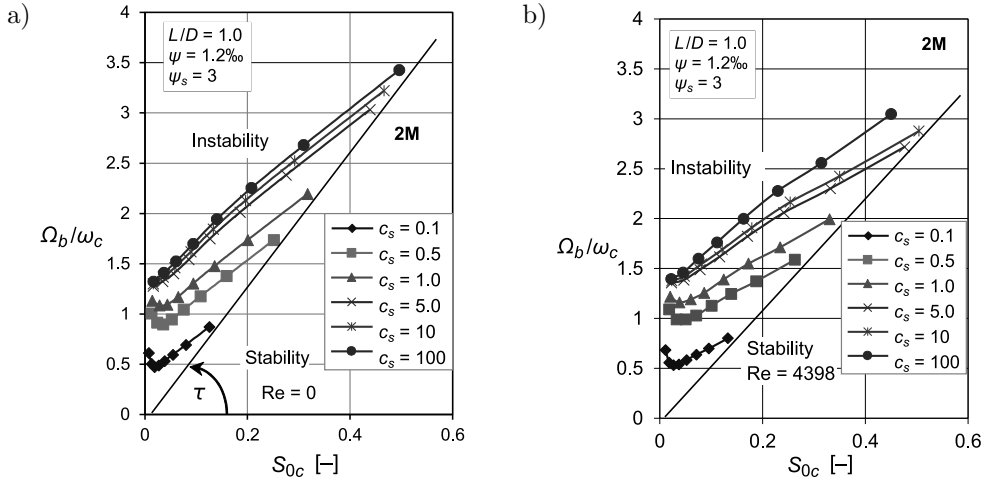


FIG. 14. Stability ranges of a two-lobe journal bearing (2M) versus the critical Sommerfeld number.

5. FINAL REMARKS

The design of journal bearings for high-speed rotating machines should be carried out with the use of algorithms that account for the phenomenon of local transition between laminar and turbulent oil flow in the bearing lubricating gap. This transition, which is generated by increased rotational speed, reduced load, or changes in lubricant viscosity, impacts the dynamic characteristics of the bearings.

This study presented a theoretical investigation into the dynamic characteristics of selected two-lobe journal bearings working under both laminar and turbulent oil film conditions. The lobes of equal geometry characterize the considered bearings.

The dynamic characteristics, specifically in the stiffness and damping coefficients of the oil film of the two-lobe journal bearings with different sleeve profiles, were computed using a developed numerical algorithm. The results provided input data for the investigation and analysis of bearing stability across various multilobe journal bearings.

The relationship between journal relative eccentricity and the Sommerfeld number shows that an increase in relative eccentricity leads to greater load capacity under turbulent oil film conditions.

Notably, the multilobe journal bearings 2M, 2OF and 2P exhibit higher values for the stiffness g_{22} and damping b_{22} coefficients under turbulent conditions than under the laminar case conditions. Conversely, for the 2C bearing, these coefficients are larger in the laminar oil film conditions.

Furthermore, an increase in the relative elasticity of the rotor enhances the rotor stability for both laminar and turbulent oil film conditions.

Overall, it was shown that turbulence has an effect on the static and dynamic characteristic as well as the stability of rotors operating in the considered journal bearings. This fact opens new possibilities for investigating the challenges in the design of high-speed bearings.

REFERENCES

1. PINKUS O., *Thermal Aspects of Fluid Film Tribology*, ASME, 1990.
2. SOMEYA T., *Journal-Bearing Databook*, Springer-Verlag, Berlin, Heidelberg, 1989.
3. HAN D.C., *Static and Dynamic Properties of Plain Bearings at High Circumferential Speeds and Tilting* [in German: *Statische und dynamische Eigenschaften von Gleitlagern bei hohen Umfangsgeschwindigkeiten und bei Verkantung*], Ph.D. thesis, TU Karlsruhe, 1979.
4. DETTMAR D., KÜHL S., *et al.*, Advancement of a radial journal bearing for highest load capacity for big steam turbines for power generation, *7th IFToMM Conference on Rotor Dynamics*, September 25–28, Vienna, Austria, 2006.
5. HOPF G., SCHÜLER D., Investigations on large turbine bearings working under transitional conditions between laminar and turbulent flow, *Journal of Tribology*, **111**(4): 628–634, 1989, <https://doi.org/10.1115/1.3261987>.
6. STRZELECKI S., Effect of turbulent oil film on the operating characteristics of 4-lobe journal bearing, [in:] *Proceedings of the 11th Nordic Symposium on Tribology NORDTRIB 2004*, Tromsø-Harstad-Hurtigruten, Norway, June 2004, pp. 177–186, 2004.
7. STRZELECKI S., Power loss of tilting 5-pad journal bearing operating with turbulent oil film, *Synopses of 3rd World Tribology Congress*, September 12–16, 2005, Washington, DC, 2005.
8. GLIENICKE J., HAN D-C., LEONHARD M., Properties of plain bearings at high circumferential speeds [in German: *Eigenschaften von Gleitlager bei hohen Umfangsgeschwindigkeiten*], *Konstruktion*, **33**: 441–448, 1981.
9. NG C.-W., PAN C.H.T., A linearized turbulent lubrication theory, *Journal of Basic Engineering*, **87**(3): 675–682, 1965, <https://doi.org/10.1115/1.3650640>.
10. HIRS G.G., A bulk-flow theory for turbulence in lubricant films, *Journal of Lubrication Technology*, **95**(2): 137–145, 1973, <https://doi.org/10.1115/1.3451752>.
11. TAYLOR C.M., DOWSON D., Turbulent lubrication theory-application to design, *Journal of Lubrication Technology*, **96**(1): 36–46, 1974, <https://doi.org/10.1115/1.3451905>.
12. STRZELECKI S., *Journal Bearings. Identification of the Operating Characteristics of Multilobe, Hydrodynamic Radial Bearings* [in Polish], Publishing House of the Silesian University of Technology, Gliwice, Poland, 2021.
13. KRAMER E., *Machine Dynamics* [in German: *Maschinendynamik*], Springer-Verlag, Berlin, Heidelberg, 1984.

14. STRZELECKI S., Calculation of journal bearing with turbulent oil film, [in:] *Proceedings of the VIth International Symposium on Tribology INTERTRIBO'99*, April 27–30, 1999, Stara Lesna, The High Tatras, Slovakia, pp. 471–474, 1999.
15. STRZELECKI S., Effect of turbulence on the dynamic characteristics of 3-lobe journal bearing, *Tribologia*, **5**: 665–676, 1999.
16. STRZELECKI S., Dynamic characteristics of tilting 5-pad journal bearing at turbulent oil film, [in:] *Proceedings of the 3rd International Symposium on Stability Control of Rotating Machinery (ISCORMA)*, pp. 242–249, September 19–23, 2005, Cleveland, OH, CD Edition, 2005.

Received December 7, 2024; accepted version February 7, 2025.

Online first May 13, 2025..
